Article

Gas-Phase Catalytic Dehydration of Glycerol with Methanol to Methyl Glyceryl Ethers over Phosphotungstic Acid Supported on Alumina

Guangxin Jia,* Ye Zhang, Laishuan Liu, Yu Li, and Baoliang Lv

Read Online

ACCESS | Metrics & More | Article Recommendations

ABSTRACT: Glycerol can be dehydrated with methanol to produce methyl glyceryl ethers as biologicals and diesel fuel additives. Considering the high efficiency of mass transfer and product separation in the gas−solid catalytic process, a fixed-bed continuous-flow reactor was used to carry out the catalyst evaluation test of the process at 564 K. Compared with zirconium sulfate, lanthanum nitrate, and ammonium molybdate, phospho-tungstic acid exhibits a higher target product selectivity. Through loading experiments, it was found that the optimal loading fraction of phosphotungstic acid on alumina is 10 wt %. After the alumina carrier is impregnated with nitric acid, the selectivity and yield of monomethyl glycerol ether can be effectively improved, and it has little effect on other products. A test of the addition amount of cerium nitrate as a promoter was carried out. It was shown in the test that when the addition amount of cerium nitrate is 10 wt %, the catalyst life increases from 2 to 3.5 h and the selectivity of dimethyl glycerol ether increases to 54.51%, which is twice the original. However, the selectivities of monomethyl glycerol ether and trimethyl glycerol ether decrease by one-half each. Through catalyst characterization, it was shown that carbon deposition on the catalyst surface is one of the reasons for catalyst deactivation.
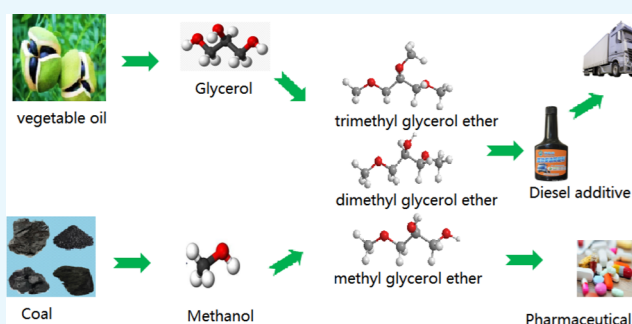
1. INTRODUCTION

Due to the overexploitation and continuous consumption of petroleum resources, clean renewable alternative energy has attracted more and more attention. Among all renewable energies, biodiesel has been widely used in recent years due to its unique combustion and blending properties. However, its synthesis process through the transesterification reaction produces glycerol with a mass fraction of 10%. In view of this, the development of high value-added derivatives for glycerol has been attracting a lot of attention from researchers.[1−3]

Among all glycerol derivatives, alkyl glycerol ethers have attracted much attention. Alkyl glyceryl ethers are a mixture of monoalkyl glyceryl ether (MAGE), dialkylglyceryl ether (DAGE), and trialkyl glyceryl ether (TAGE) prepared by the dehydration of glycerol and monohydric alcohols.

MAGE can be applied in immunostimulatory, antimicrobial, and antitumor applications and anesthesia due to its special biological characteristics.[4] Moreover, it can be used as additives in drugs,[5,6] cosmetics,[7] liquid detergents,[8] herbicides,[9] lubricants,[10] and solvents.[11] DAGE and TAGE can be used as fuel additives for diesel, biodiesel, and ethanol gasoline, which can effectively improve fuel quality and reduce pollutant emissions of respirable particles, hydrocarbons, carbon monoxide, and unregulated aldehydes.[12−15]

Alkyl glycerol ethers can be synthesized by etherification of glycerol with isobutene and dehydration of glycerol with alcohols such as tert-butyl alcohol, ethanol, and methanol.[16] The etherification process of glycerol with isobutene is limited because of isobutene self-polymerization.[17,18] In view of low cost and wide source of raw materials, the dehydration of glycerol with alcohol has more advantages.[19,20]
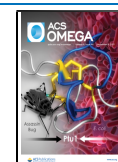
The dehydration process of glycerol with alcohols is shown in Figure 1.

As seen in Figure 1, there are three consecutive reversible reactions catalyzed by the acid. Most researchers focus on the preparation and development of the catalyst but ignore the evaluation process of the catalyst. Because most catalyst evaluations are carried out in closed stirred reactors,[21−23] they lead to a dilemma: the higher the catalyst activity, the
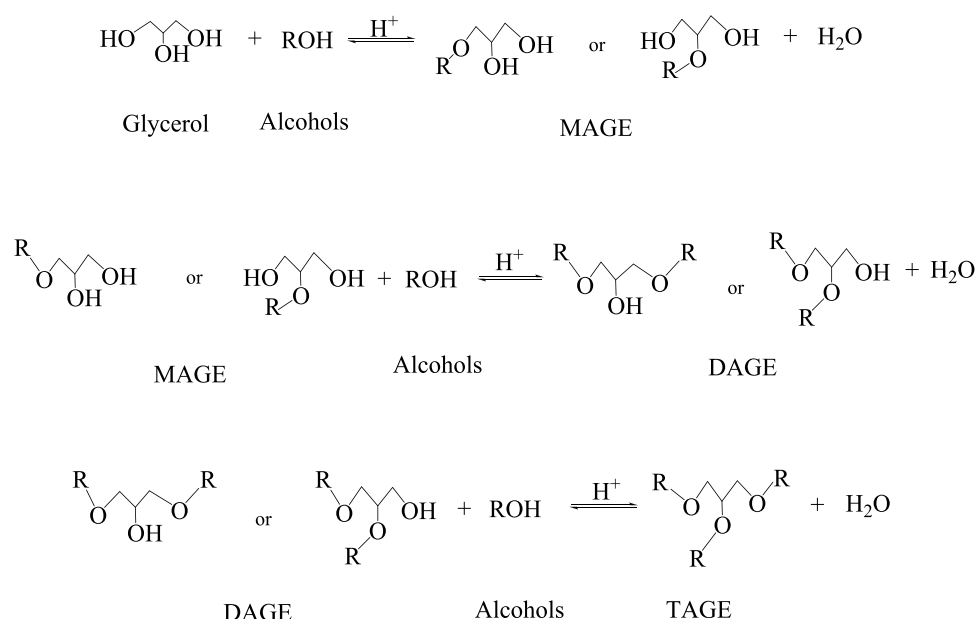
Figure 1. Dehydration process of glycerol with alcohols.

Table 1. Effect of Impregnation Components on Catalyst Performance

impregnation component	reaction time (h)	glycerol conversion (%)	selectivity (%)				
			MMGE	DMGE	TMGE	MMGE + DMGE + TMGE	byproducts
zirconium sulfate	0.5	91.6	22.0	10.2	6.7	38.9	61.1
	1	72.4	6.9	3.6	4.8	15.3	84.7
lanthanum nitrate	0.5	65.1	4.4	3.9	4.9	13.2	86.8
	1	35.1	4.1	2.9	1.4	8.4	91.6
ammonium molybdate	0.5	91.7	2.5	5.1	10.8	18.4	81.6
	1	87.6	19.5	24.6	9.8	53.9	46.1
	1.5	43.3	9.6	5.3	0.9	15.8	84.2
HPW	0.5	90.1	22.1	28.7	16.7	67.5	32.5
	1	91.7	18.1	28.4	23.3	69.8	30.2
	1.5	86.2	10.7	11.0	13.8	36.1	63.9
	2	78.1	1.1	2.6	2.0	5.70	94.3

more water will be generated. However, this excess water, in turn, leads to catalyst deactivation. Therefore, only when the reaction system is in a continuous-flow reaction state is it possible to eliminate this dilemma. At present, few research studies that involved dehydration of glycerol with alcohols in a fix-bed reactor have been reported.[24−27] Since the boiling point of glycerol is as high as 564 K, the reaction temperature must be maintained at least at 564 K. Under these conditions, the better catalyst in closed reaction tank, such as ion exchange resin, is completely unusable.[28−30]

Based on the above analysis, the development of a more efficient and stable catalyst suitable for a fixed-bed reactor has become the key to the synthesis of alkyl glycerol ethers. In recent studies, some supported phosphotungstic acid (HPW) catalysts presented superior catalytic activity in other dehydration reactions.[31−34]

In this article, the gas-phase dehydration reaction process of glycerol and methanol was carried out in a fixed bed. The focus is on the catalytic behavior of acid catalysts including HPW on the synthesis of alkyl glycerol ethers. It is expected that this research will provide help and support for the follow-up research on alkyl glycerol ethers.

2. RESULTS AND DISCUSSION

2.1. Effect of Different Impregnation Components on Catalyst Performance. Under the condition of pretreated commercial alumina as the carrier, the effect of different impregnation components on catalyst performance was evaluated in the fix-bed reactor at 564 K, a 6:1 molar ratio of methanol-to-glycerol, a feed flow rate of 0.14 mL· min^{-1}, and 3.0 g of the catalyst. Zirconium sulfate, cerium nitrate, ammonium molybdate, and HPW were employed as impregnation components. As the target products of the reaction, monomethyl glyceryl ether, dimethyl glyceryl ether, and trimethyl glyceryl ether are abbreviated as MMGE, DMGE, and TMGE, respectively. The results are shown in Table 1.

It can be seen from Table 1 that there is a great difference in the catalytic effects of the four impregnation components. Overall, the glycerol conversion ranges from 35.1 to 91.7%, while MMGE + DMGE + TMGE selectivities range from 5.7 to 69.8%. It is worth noting that glycerol conversions and MMGE + DMGE + TMGE selectivities for the HPW catalyst reached 91.7 and 69.8%, respectively, at 1 h. Under this condition, the selectivities of MMGE, DMGE, and TMGE are 18.1, 28.4, and 23.3%, respectively. It is proved by the
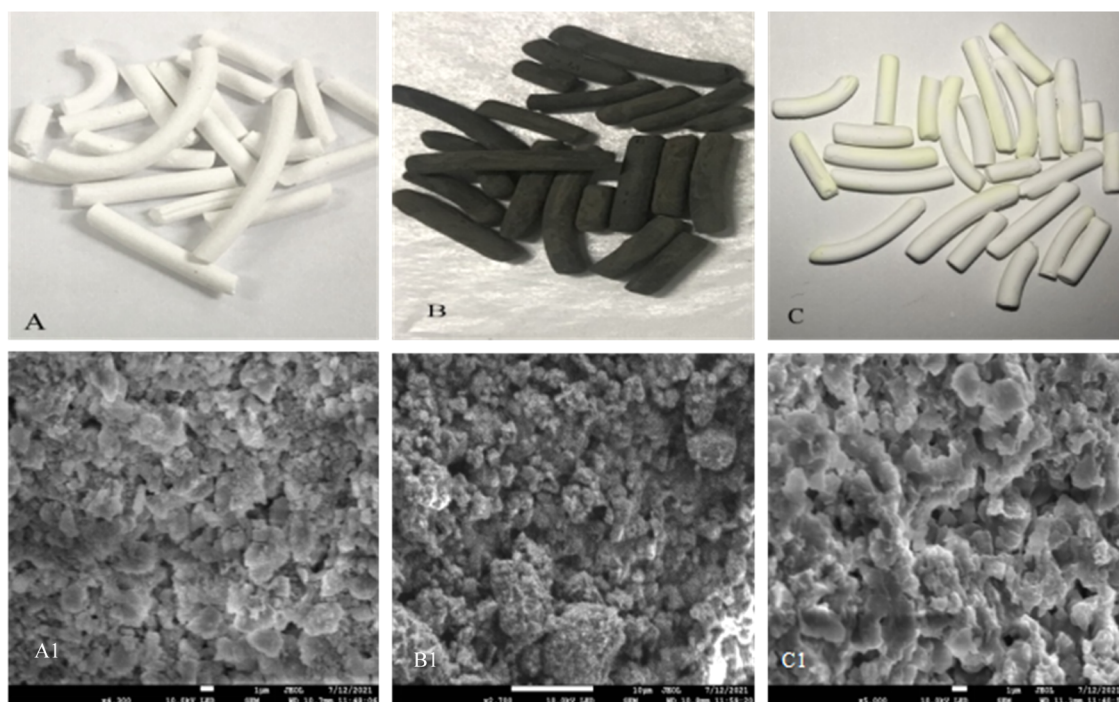
Figure 2. (A) Photo of the HPW/Al$_2$O$_3$ catalyst before reaction; (B) photo of the HPW/Al$_2$O$_3$ catalyst after use; and (C) photo of the catalyst calcined at 773 K for the used HPW/Al$_2$O$_3$. (A1) SEM image of the HPW/Al$_2$O$_3$ catalyst before reaction; (B1) SEM image of the HPW/Al$_2$O$_3$ catalyst after use; (C1) SEM image of the catalyst calcined at 773 K for the used HPW/Al$_2$O$_3$.

data that phosphotungstic acid is a more suitable catalyst for the dehydration reaction of glycerol and methanol, which is consistent with the reports in the literature reported by Sakthivel.[35]

As shown in Table 1, although HPW presents excellent initial activity, the glycerol conversion decreases sharply with time, and the byproduct occupies an absolute majority at 2 h. According to gas chromatography-mass spectrometry analysis, the byproducts of the reaction system not only contain dimethyl ether but also include acrolein, cycloacetone, methacrylate, glycidol, and 3-hydroxypropionaldehyde. Their mole fractions are directly related to the catalyst composition, preparation method, reaction temperature, and feed composition.

The photos showing the appearance and scanning electron microscope (SEM) images of HPW catalysts are shown in Figure 2.

As shown in Figure 2A,B, the catalyst exhibits an obvious color change from white to black after the reaction. However, as shown in Figure 2C, the catalyst becomes white again when calcined at 773 K for 2 h.

Compared with Figure 2A1,B1, it can be seen that before the reaction, the HPW distribution in the catalyst is relatively uniform and the particles are larger. However, after the catalyst is used, the particles become finer and the surface morphology is rough. It is shown that the catalyst surface is covered by a substance, which causes catalyst deactivation. After the reacted catalyst was calcined at 773 K, the surface of the catalyst became clear and the particles became larger again. This change is more like a process in which deposited carbon is formed on the catalyst surface and then the deposited carbon disappears. This phenomenon is consistent with the carbon deposition process reported in the literature.[36]

To further reveal the difference between the phosphotungstic acid catalyst before and after the reaction, the X-ray diffraction (XRD) characterization of the three samples was performed. The corresponding spectrum is shown in Figure 3.

It can be seen from Figure 3 that the diffraction peak intensity of the phosphotungstic acid crystal phase reflects the dispersion of the phosphotungstic acid on the carrier. When 2θ is 8.5 and 23.6°, the angles of the diffraction peaks before and after the reaction are the same but the intensities are different. This may be due to the fact that the active sites of
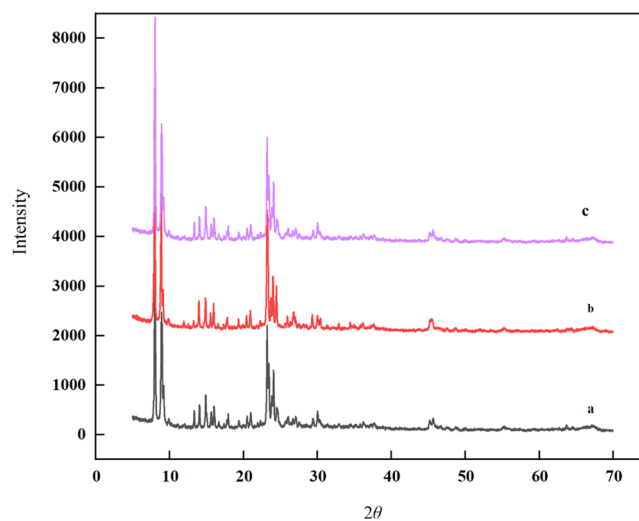
Figure 3. (a) XRD spectrum of the unreacted HPW/Al$_2$O$_3$ catalyst. (b) XRD spectrum of the HPW/Al$_2$O$_3$ catalyst after the reaction. (c) XRD spectrum of the HPW/Al$_2$O$_3$ catalyst after recalcination at 773 K.
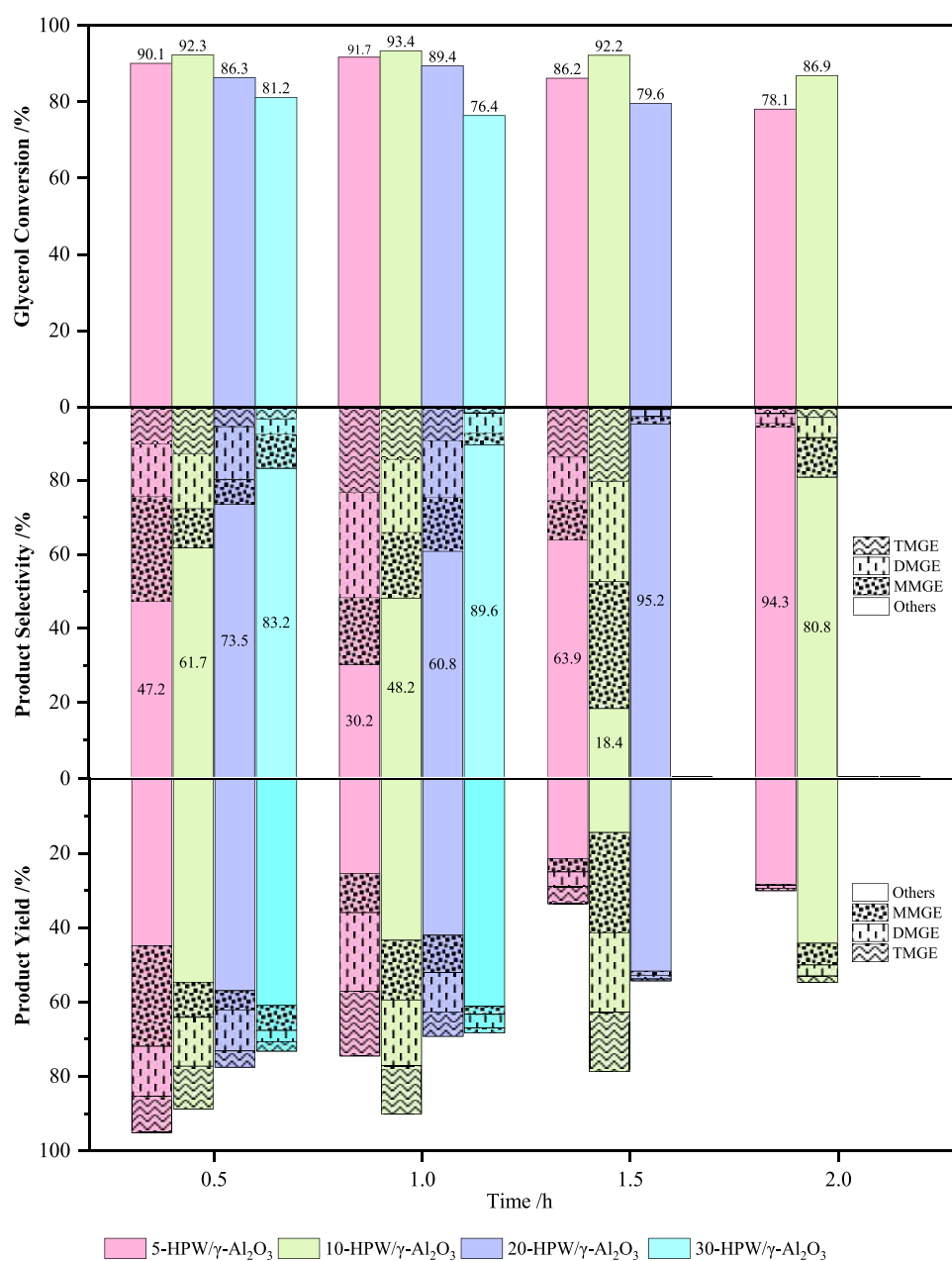
Figure 4. HPW loading investigation on glycerol dehydration with methanol.

the catalyst are covered by deposited carbon after the reaction. The diffraction peak intensity of the catalyst after calcination at 773 K increases but the angle remains unchanged. This phenomenon indicates that the reaction and calcination process did not damage the framework structure of the catalyst, the charge balance of the procatalyst can still be maintained, and the structure of the procatalyst is not destroyed.

Since the catalyst life is only 2 h, the catalyst deactivation may not only be related to carbon deposition but also be related to the loss of active components caused by the surface of the phosphoric acid catalyst with water.[32]

2.2. Effect of HPW Loading on Catalyst Performance. The HPW loading investigation on glycerol dehydration with methanol was carried out over 5-HPW/γ-Al$_2$O$_3$, 10-HPW/γ-Al$_2$O$_3$, 20-HPW/γ-Al$_2$O$_3$, and 30-HPW/γ-Al$_2$O$_3$ catalysts at 564 K, a 6:1 molar ratio of methanol-to-glycerol,

a feed flow rate of 0.14 mL·min^{-1}, and 3.0 g of catalyst. The results are given in Figure 4.

The complex relationship between glycerol conversion, product selectivity, yield, and catalyst life as the HPW loading increases is shown in Figure 4. The abscissa in Figure 4 represents the reaction time of 0.5, 1.0, 1.5, and 2.0 h. The results of the HPW loading investigation were placed in sequence near these four time points for comparison.

By comparing the background data in Figure 4, it can be seen that the 10-HPW/γ-Al$_2$O$_3$ catalyst at 1.5 h shows the best catalytic results in all experiments, that is, the selectivities of MMGE, DMGE, and TMGE were 34.2, 27.1, and 20.3%, the total ether selectivity reaches 81.6%, and the byproducts are the least. However, when the HPW loading amount was increased to 20 and 30%, the glycerol conversion and product selectivity dropped significantly and the catalyst life also reduced to 1.5 and 1 h, respectively, from
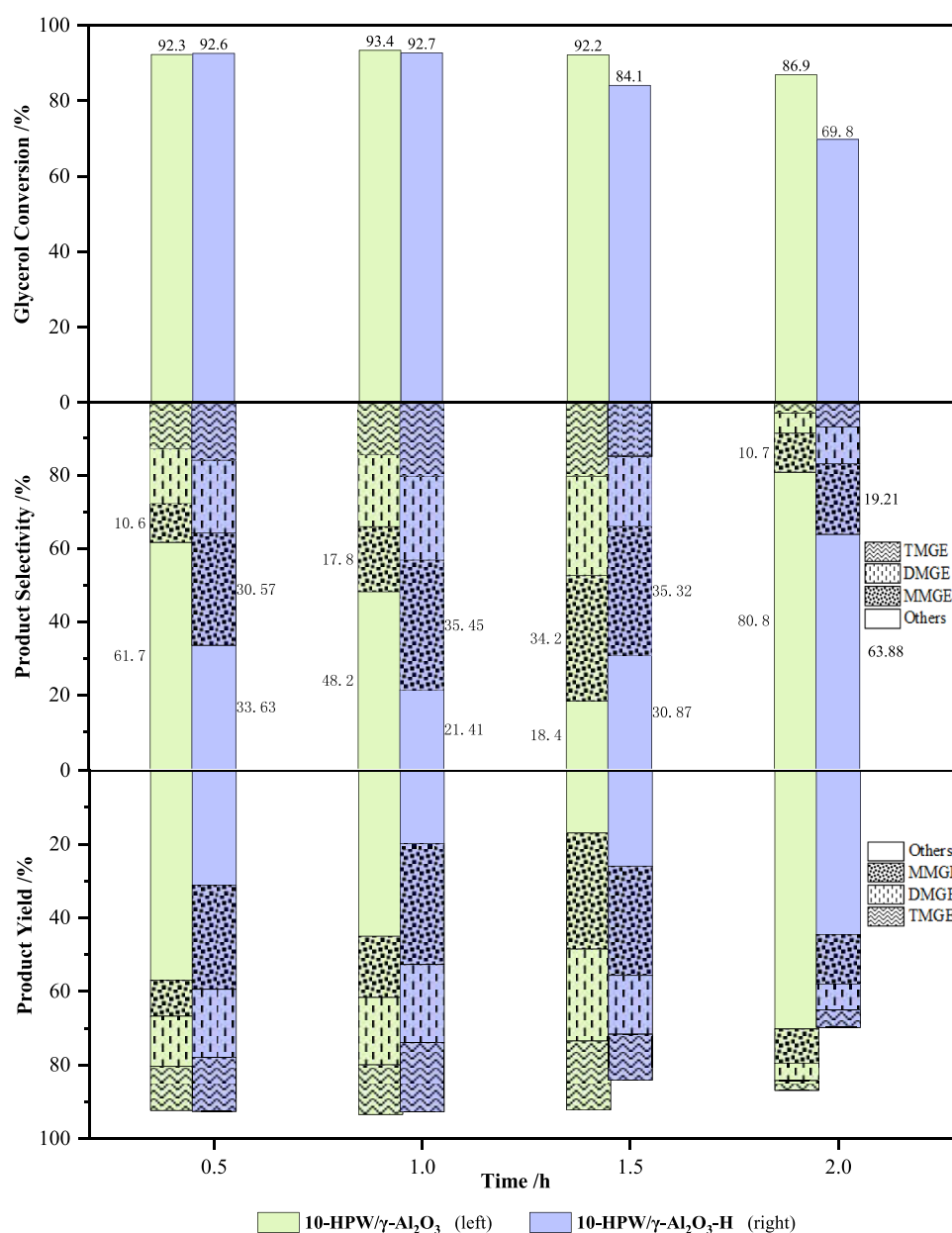
Figure 5. Comparison of HPW/γ-Al$_2$O$_3$ before and after treatment with nitric acid.

2 h at 10% loading. This shows that 10% loading is the best and that too low or too high loading will affect the catalytic performance. The reason could be that when the loading is less than 10%, the catalyst is covered by a monomolecular layer on the catalyst surface. The smaller the loading, the smaller the surface area covered by the active components. When the loading is greater than 10%, the surface of the catalyst gradually begins to be a multimolecular layer covering, which blocks the surface of the carrier to a certain extent. This directly leads to the following results: the larger the catalyst loading, the smaller the surface area covered by the active components.

However, the catalyst life of only 2 h is far from enough for a normal experiment and follow-up research. The improvement research needs to be carried out from the two aspects of catalyst carrier pretreatment and cocatalyst addition.

2.3. Influence of Carrier Impregnation with Nitric Acid. To improve the structure of the carrier surface and make it more suitable for the loading process, the catalyst carrier was impregnated with dilute nitric acid before loading. This experiment was carried out on the basis of the previous HPW loading investigation. Therefore, the loading weight ratio of HPW and γ-Al$_2$O$_3$ is determined to be 10%, and the process of nitric acid impregnation of alumina belongs to excessive impregnation.

The comparison experiments before and after treatment with nitric acid were carried out at 564 K, a 6:1 molar ratio of methanol-to-glycerol, a feed flow rate of 0.14 mL·min^{-1}, and 3.0 g of the catalyst. The catalyst pretreated with nitric acid is labeled 10-HPW/γ-Al$_2$O$_3$-H, and the catalyst without pretreatment is labeled 10-HPW/γ-Al$_2$O$_3$. The results are illustrated in Figure 5.

It can be seen from Figure 5 that the glycerol conversion after nitric acid treatment of the carrier only increased slightly

Table 2. Effect of Cerium Nitrate Loading on the Catalytic Performance

impregnation component	reaction time (h)	glycerol conversion (%)	selectivity (%)				
			MMGE	DMGE	TMGE	MMGE + DMGE + TMGE	byproducts
10-HPW/γ-Al₂O₃	0.5	92.3	10.60	14.80	12.90	38.30	61.70
	1	93.4	17.80	19.60	14.40	51.80	48.20
	1.5	92.2	34.2	27.10	20.30	81.60	18.40
	2	86.9	10.7	5.40	3.10	19.20	80.80
10-HPW/γ-Al₂O₃-Ce5	0.5	90.2	8.17	15.85	1.79	25.81	74.18
	1	99.2	15.74	19.83	4.09	39.66	60.34
	1.5	80.3	33.84	20.31	3.38	57.53	42.47
	2	60.9	18.65	9.81	1.51	29.97	70.03
10-HPW/γ-Al₂O₃-Ce10	0.5	94.9	11.9	25.26	2.86	40.02	59.97
	1	90.9	15.06	37.25	5.40	57.71	42.29
	1.5	92.4	15.87	54.51	7.17	77.55	22.44
	2	94.1	10.8	43.85	8.24	62.89	37.11
	2.5	90.3	9.43	39.37	2.64	51.44	48.55
	3	69.6	2.78	22.67	1.22	26.67	73.38
	3.5	39.4	1.97	8.60	0.70	11.27	88.72
10-HPW/γ-Al₂O₃-Ce20	0.5	82.8	13.81	12.40	6.00	32.21	67.79
	1	83.4	12.26	9.80	6.92	28.98	71.02
	1.5	39.1	10.34	7.79	3.73	21.86	78.13
	2	30.1	1.83	1.91	0.68	4.42	95.57
10-HPW/γ-Al₂O₃-Ce30	0.5	81.9	14.44	11.22	4.30	29.96	70.03
	1	97.9	18.71	6.28	2.24	27.23	72.77
	1.5	39.6	8.95	5.17	0.70	14.82	85.17
	2	29.9	1.89	1.86	0.67	4.42	95.57

at the time point of 0.5 h, while the glycerol conversion began to decrease after 1.0 h. It is worth noting that the nitric acid treatment of the carrier catalyst significantly improved the selectivity of MMGE. However, the selectivities and yields for DMGE and TMGE increase very little or even decrease slightly.

It was shown from the experiments that the surface structure of the alumina pretreated by nitric acid is beneficial to the first-step dehydration process between more glycerol and methanol molecules.

According to the analysis and characterization results of nitric acid impregnation of vermiculite for alcohol dehydration in the literature, it can be considered that the treatment of alumina with nitric acid may bring about two results: first, the specific surface area and pore volume of the support are significantly increased, and second, the Al^{3+} cations in the pores are partially leached.[37] The increase of pore volume and specific surface area is beneficial for more methanol and glycerol molecules to enter the pores and be adsorbed and activated, while the leaching of Al^{3+} cations will weaken the acid density of the pore surface to a certain extent. This will directly lead to an increase in the content of monomethyl glyceryl ether but a decrease in the content of dimethyl ether and trimethyl glyceryl ether. The experimental results are basically consistent with the alcohol dehydration results reported in the literature.[37]

2.4. Influence of Carrier Impregnation with Cerium Nitrate. To improve the catalytic performance of the phosphotungstic acid catalyst, a loading test of cerium nitrate as a cocatalyst was carried out on the basis of the 10-HPW/γ-Al₂O₃ catalyst. The catalysts are 10-HPW/γ-Al₂O₃, 10-HPW/γ-Al₂O₃-Ce5, 10-HPW/γ-Al₂O₃-Ce10, 10-HPW/γ-Al₂O₃-Ce20, and 10-HPW/γ-Al₂O₃-Ce30. The loading test was carried out under the condition of 564 K, the 6:1 molar ratio

of methanol-to-glycerol, a feed flow rate of 0.14 mL·min⁻¹, and 3.0 g of the catalyst. The results are shown in Table 2.

It can be seen from Table 2 that when the loading amount of cerium nitrate is 10%, the reaction time for maintaining the glycerol conversion above 90% is extended to 2.5 from 1.5 h and the total reaction time is extended to 3.5 from 2 h. Although the selectivity of the MMGE + DMGE + TMGE decreased to a certain extent, the total selectivity of dimethyl glycerol ether and trimethyl glycerol was higher than that of unsupported cerium nitrate under the same conditions, and the selectivity of dimethyl glycerol is far greater than that of trimethyl glycerol.

From the comparison data of cerium nitrate loading in Table 2, it can be seen that the optimal loading of cerium nitrate is 10%. Both trace and excess amounts will affect the catalytic performance of cerium nitrate. A small amount of cerium nitrate will not have the proper catalytic effect, while excessive cerium nitrate will affect the catalytic performance of the main catalyst due to excessive occupation of active sites.[38]

To reveal the influence of the addition of cerium nitrate on the reaction, the NH₃-TPD characterization of different supported catalysts was carried out. The specific spectrum is shown in Figure 66.

The results showed that most of the catalysts show weak (423−573 K) and medium (573−773 K) acid site desorption peaks. It can be roughly seen from the relative integrated area of the spectral peaks that as the loading of cerium nitrate increases, the amount of acid at the weak acid sites gradually decreases, while the strong acid sites change slightly. It was shown that the lower content of cerium nitrate is beneficial to the reaction process. From the comparison of 5 and 10% content of cerium nitrate loading, it can be found that the 10% content of cerium nitrate catalyst contains a small part of strong acid sites, which leads to a significant increase in
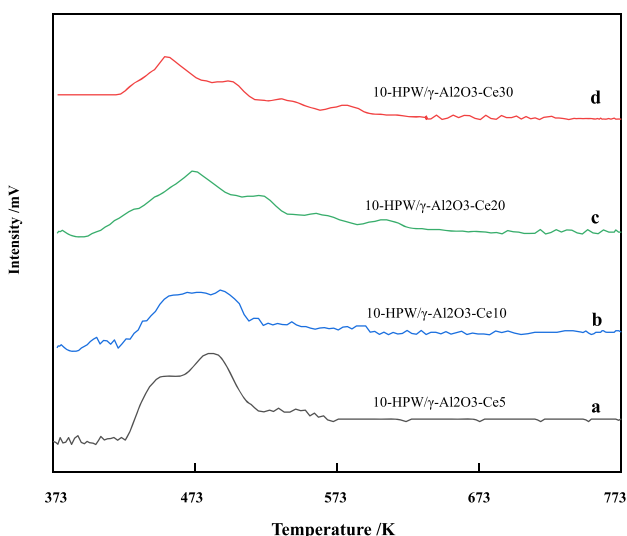
Figure 6. (a) NH$_3$-TPD spectra of 10-HPW/γ-Al$_2$O$_3$-Ce5, (b) 10-HPW/γ-Al$_2$O$_3$-Ce10, (c) 10-HPW/γ-Al$_2$O$_3$-Ce20, and (d) 10-HPW/γ-Al$_2$O$_3$-Ce30.

the selectivity of dimethyl glycerol ether. These analysis results are basically consistent with the conclusions of the literature.[39,40]

3. CONCLUSIONS

Compared with zirconium sulfate, cerium nitrate, and ammonium molybdate, phosphotungstic acid is more suitable as an active component in the catalytic dehydration process of glycerol and methanol. Through the load test of phosphotungstic acid on alumina, it was found that when phosphotungstic acid is loaded on alumina at a weight ratio of 10%, it shows the best catalytic results. Considering that the catalyst life is only 2 h, the improvement is made by two means: carrier pretreatment and cocatalyst addition. The results showed that the selectivity of monomethyl glycerol ether was greatly improved after γ-Al$_2$O$_3$ was pretreated with nitric acid. After adding cerium nitrate at a mass ratio of 10%, the total selectivity of dimethyl ether, glycerol ether, and trimethyl glycerol ether was significantly increased, the selectivity of monomethyl glycerol ether was reduced, and the catalyst life was extended to 3.5 from 2 h.

4. EXPERIMENTAL SECTION

4.1. Chemical Reagents and Materials. All chemical reagents used in this work were of analytical reagent (AR) grade. Glycerol (Tianjin Fuyu Fine Chemical Co., Ltd.), methanol (Tianjin Chemical Reagent Plant), cerium nitrate (Shanghai Boer Chemical Reagents Co., Ltd.), phosphotungstic acid (H$_3$PW$_{12}$O$_{40}$) (Shanghai Zhanyun Chemical Co., Ltd.), p-toluene sulfonic acid (Tianjin Kaitong Chemical Reagents Co., Ltd.), zirconium sulfate/lanthanum nitrate (Tianjin Guangfu Fine Chemical Research Institute), nitric acid (HNO$_3$) (Tianjin Yaohua Chemical Reagent Co., Ltd.), ammonium molybdate (Tianjin Chemical Reagent Plant), and commercial alumina (Zibo Chaoke alumina materials Co., Ltd.) were obtained.

4.2. Carrier Preparation. Commercial alumina (γ-Al$_2$O$_3$) was obtained by calcining commercial alumina in a muffle furnace at 823 K for 10 h.

4.3. Impregnation of Different Impregnation Components. Ten grams of alumina was impregnated with zirconium sulfate, cerium nitrate, ammonium molybdate, and HPW aqueous solution separately as 5 wt % to obtain the four impregnated precursors, and then those precursors were placed in vacuum at 393 K for 5 h and finally calcined at 773 K for 6 h in a muffle furnace.

4.4. HPW Loading Investigation. Ten grams of alumina was impregnated with HPW aqueous solution as 5, 10, 20, and 30 wt % and then calcined at 773 K for 6 h to obtain the catalyst samples: 5-HPW/γ-Al$_2$O$_3$, 10-HPW/γ-Al$_2$O$_3$, 20-HPW/γ-Al$_2$O$_3$, and 30-HPW/γ-Al$_2$O$_3$, respectively.

4.5. Nitric Acid Treatment of the Carrier. Concentrated nitric acid (HNO$_3$) (68 wt %) was diluted to 17 wt %. After that, the γ-Al$_2$O$_3$ was impregnated with HNO$_3$ (17 wt %) under stirring for 3 h at 333 K, filtered and washed with deionized water to neutrality, and then calcined at 393 K to remove the water on the surface. The HPW loading experiment was carried out according to the method mentioned in the previous section to obtain the pretreated carrier: HPW/γ-Al$_2$O$_3$-H.

4.6. Cerium Nitrate Treatment of the Carrier. Alumina was treated with cerium nitrate aqueous solutions as 5, 10, 20, and 30 wt % with stirring at 333 K for 3 h and then calcined at 773 K for 6 h in the furnace to obtain the following: γ-Al$_2$O$_3$-Ce5, γ-Al$_2$O$_3$-Ce10, γ-Al$_2$O$_3$-Ce20, and γ-Al$_2$O$_3$-Ce30. The above carriers were impregnated with HPW as 10 wt % and stirred at 333 K for 3 h and then calcined at 773 K for 6 h in a muffle furnace. Thus, the modified catalyst was prepared and named 10-HPW/γ-Al$_2$O$_3$-Ce5, 10-HPW/γ-Al$_2$O$_3$-Ce10, 10-HPW/γ-Al$_2$O$_3$-Ce20, and 10-HPW/γ-Al$_2$O$_3$-Ce30, respectively.

4.7. Synthesis of Methyl Glyceryl Ethers. The catalyst (3.0 g) was placed in the vertical cylindrical fix-bed reactor (diameter: 19 mm, length: 20 cm). The diagram of the reaction process is illustrated in Figure 7.

The feeds at a methanol-to-glycerol molar ratio of 6:1 were injected with an HPLC pump at a feed flow rate of 0.14 mL/
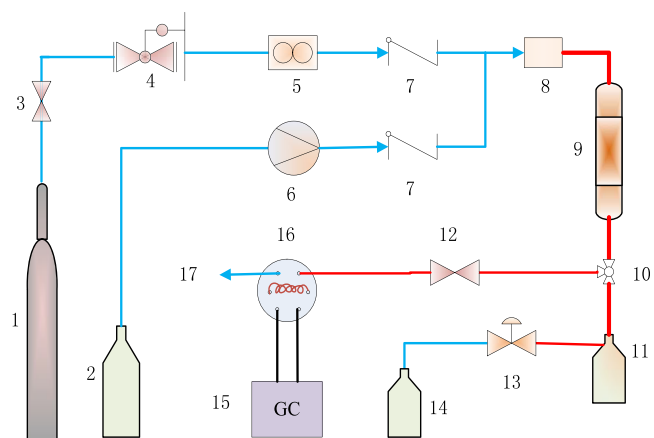
Figure 7. Diagram of the experimental setup for the dehydration of glycerol with methanol ((1) nitrogen gas cylinder; (2) feed tank; (3) cutoff valve; (4) pressure reducing value; (5) flow indicator control (FIC); (6) HPLC pump; (7) check valve; (8) preheater; (9) fixed-bed reactor; (10) three-way valve; (11) gas−liquid separator; (12) flow control valve; (13) back pressure valve; (14) volatile component tank; (15) gas chromatography; (16) six-way valve; and (17) vent).
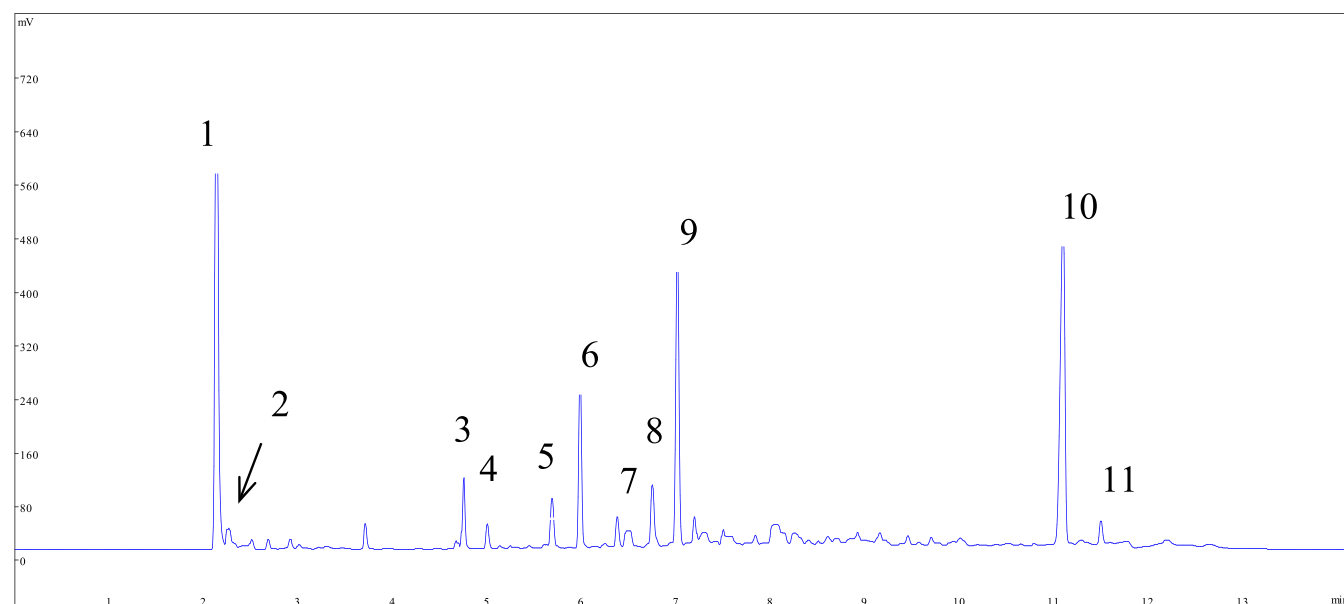
Figure 8. Typical gas chromatographic composition spectrum ((1) dimethyl ether; (2) methanol; (3) acrolein; (4) cycloacetone; (5) methacrylate; (6) trimethyl glyceryl ether; (7) glycidol; (8) 3-hydroxypropionaldehyde; (9) dimethyl glyceryl ether; (10) monomethyl glyceryl ether; and (11) glycerol).

min in a N_2 flow (10 mL/min) through the preheater and reactor. The preheater and the reactor temperatures were set at 558 and 564 K, respectively. Furthermore, the pipe highlighted in red was insulated by a heater band. N_2 was used as a carrier gas to ensure that the reactants and products can be transported more fluently. The samples were injected on-line or off-line through a three-way ball valve switch and analyzed with the flame ionization detector (FID) in a gas chromatograph (Shimadzu, GC5890) equipped with a capillary column (WONACAP 5.30 m × 0.32 mm × 0.25 μm). Methanol, glycerol, monomethyl glycerol ether, and dimethyl ether were bought, and their retention times could be confirmed. The retention times of other samples were determined by the GC−MS on the same column and under the same test conditions. The confidence level of the components tested by mass spectrometry was more than 85%.

The samples were analyzed with the temperature programmed as follows: 323 K for 2 min, heating at 30 K/min until 513 K, with 2 min of hold time, and then heating at 35 K/min to 573 K and holding for 5 min. A typical gas chromatographic composition spectrum is shown in Figure 8.

The glycerol conversion, product selectivity, and product yield were calculated as follows:

glycerol conversion (%)

$$= \text{mole of glycerol reacted/mole of glycerol feed} \times 100 \quad (1)$$

product selectivity (%)

$$= \text{mole of product obtained/mole of reacted glycerol} \times 100 \quad (2)$$

$$\text{product yield (\%)} = \text{mole of product obtained} /\text{mole of reacted glycerol} \times 100 \quad (3)$$

Due to some unforeseen experimental errors, the carbon balance of all experiments in this manuscript is in the range of 98−102%.

■ AUTHOR INFORMATION

Corresponding Author

　Guangxin Jia − *School of Chemical Engineering and Technology, North University of China, Taiyuan 030051, China;* ◉ orcid.org/0000-0002-7241-9105; Email: jiaguangxin@nuc.edu.cn

Authors

　Ye Zhang − *School of Chemical Engineering and Technology, North University of China, Taiyuan 030051, China*
　Laishuan Liu − *School of Chemical Engineering and Technology, North University of China, Taiyuan 030051, China*
　Yu Li − *School of Chemical Engineering and Technology, North University of China, Taiyuan 030051, China*
　Baoliang Lv − *State Key Laboratory of Coal Conversion, Institute of Coal Chemistry, Chinese Academy of Sciences, Taiyuan 030001, China;* ◉ orcid.org/0000-0001-8288-6076

Complete contact information is available at:
https://pubs.acs.org/10.1021/acsomega.1c02891

Notes

The authors declare no competing financial interest.

■ REFERENCES

(1) Ayoub, M.; Khayoon, M. S.; Abdullah, A. Z. Synthesis of oxygenated fuel additives via the solventless etherification of glycerol. *Bioresour. Technol.* **2012**, *112*, 308−312.

(2) Jia, G. X.; Ma, W. L.; He, B. B.; Sun, Y. F.; Liu, L. S. Comparative study on catalytic dehydration of glycerol with alcohols. *J. Braz. Chem. Soc.* **2019**, *30*, 851−858.

(3) Shin, M.; Kim, J.; Suh, Y. W. Etherification of biomass-derived furanyl alcohols with aliphatic alcohols over silica-supported nickel phosphide catalysts: effect of surplus p species on the acidity. *Appl. Catal., A* **2020**, *603*, No. 117763.

(4) Koshchii, S. V. Optimization of synthesis of mono-O-methylglycerol isomers. *Russ. J. Appl. Chem.* **2002**, *75*, 1434−1437.

(5) Poleschuk, T. S.; Sultanov, R. M.; Ermolenko, E. V.; Shulgina, L. V.; Kasyanov, S. P. Protective action of alkylglycerols under stress. *Stress* **2020**, *23*, 213−220.

(6) Pinault, M.; Guimaraes, C.; Couthon, H.; Thibonnet, J.; Fontaine, D.; Chantome, A.; Chevalier, S.; Besson, P.; Jaffres, P. A.; Vandier, C. Synthesis of alkyl-glycerolipids standards for gas chromatography analysis: application for chimera and shark liver oils. *Mar. Drugs* **2018**, *16*, No. 101.

(7) Bernal-Chávez, S. A.; Perez-carreto, L. Y.; Nava-arzaluz, M. G.; Ganem-rondero, A. Alkylglycerol derivatives, a new class of skin penetration modulators. *Molecules* **2017**, *22*, No. 185.

(8) Juarez, J. F. B.; O'rourke, D.; Judge, P. J.; Liu, L.; Hodgkin, J.; Watts, A. Lipodisqs for eukaryote lipidomics with retention of viability: sensitivity and resistance to leucobacter infection linked to *C. elegans* cuticle composition. *Chem. Phys. Lipids* **2019**, *222*, 51−58.

(9) Yang, S. J.; Jan, Y. H.; Mishin, V.; Richardson, J. R.; Hossain, M. M.; Heindel, N. D.; Heck, D. E.; Laskin, D. L.; Laskin, J. D. Sulfa drugs inhibit sepiapterin reduction and chemical redox cycling by sepiapterin reductase. *J. Pharmacol. Exp. Ther.* **2015**, *352*, 529−540.

(10) Rorrer, J. E.; Bell, A. T.; Toste, F. D. Synthesis of biomass-derived ethers for use as fuels and lubricants. *ChemSusChem* **2019**, *12*, 2835−2858.

(11) Soares, B. P.; Abranches, D. O.; Sintra, T. E.; Leal-Duaso, A.; Garcia, J. I.; Pires, E.; Shimizu, S.; Pinho, S. P.; Coutinho, J. A. P. Glycerol ethers as hydrotropes and their use to enhance the solubility of phenolic acids in water. *ACS Sustainable Chem. Eng.* **2020**, *8*, 5742−5749.

(12) Pinto, B. P.; De Lyra, J. T.; Nascimento, J. A. C.; Mota, C. J. A. Ethers of glycerol and ethanol as bioadditives for biodiesel. *Fuel* **2016**, *168*, 76−80.

(13) Mardi, K. M.; Antoshkiv, O.; Berg, H. P. Experimental analysis of the effect of nano-metals and novel organic additives on performance and emissions of a diesel engine. *Fuel Process. Technol.* **2019**, *196*, No. 106166.

(14) Samoilov, V. O.; Maximov, A. L.; Stolonogova, T. I.; Chernysheva, E. A.; Kapustin, V. M.; Karpunina, A. O. Glycerol to renewable fuel oxygenates. part i: comparison between solketal and its methyl ether. *Fuel* **2019**, *249*, 486−495.

(15) Chang, J. S.; Lee, Y. D.; Chou, L. C. S.; Ling, T. R.; Chou, T. C. Methylation of glycerol with dimethyl sulfate to produce a new oxygenate additive for diesels. *Ind. Eng. Chem. Res.* **2012**, *51*, 655−661.

(16) Sutter, M.; Da Silva, E.; Duguet, N.; Raoul, Y.; Metay, E.; Lemaire, M. Glycerol ether synthesis: a bench test for green chemistry concepts and technologies. *Chem. Rev.* **2015**, *115*, 8609−8651.

(17) Lee, H. J.; Seung, D.; Jung, K. S.; Kim, H.; Filimonov, I. N. Etherification of glycerol by isobutylene tuning the product composition. *Appl. Catal., A* **2010**, *390*, 235−244.

(18) Izquierdo, J. F.; Iniesta, E.; Outon, P. R.; Izquierdo, M. Experimental study of glycerol etherification with C-5 olefins to produce biodiesel additives. *Fuel Process.Technol.* **2017**, *160*, 1−7.

(19) Samoilov, V. O.; Onishchenko, M. O.; Ramazanov, D. N.; Maximov, A. L. Glycerol isopropyl ethers: direct synthesis from alcohols and synthesis by the reduction of solketal. *ChemCatChem* **2017**, *9*, 2839−2849.

(20) Samoilov, V. O.; Maximov, A. L.; Stolonogova, T. I.; Chernysheva, E. A.; Kapustin, V. M.; Karpunina, A. O. Glycerol to renewable fuel oxygenates. Part I: Comparison between solketal and its methyl ether. *Fuel* **2019**, *249*, 486−495.

(21) Melero, J. A.; Vicente, G.; Paniagua, M.; Morales, G.; Munoz, P. Etherification of biodiesel-derived glycerol with ethanol for fuel formulation over sulfonic modified catalysts. *Bioresour. Technol.* **2012**, *103*, 142−151.

(22) Kumari, U.; Behera, S. K.; Siddiqi, H.; Meikap, B. C. Facile method to synthesize efficient adsorbent from alumina by nitric acid activation: batch scale defluoridation, kinetics, isotherm studies and implementation on industrial wastewater treatment. *J. Hazard. Mater.* **2020**, *381*, No. 120917.

(23) Jia, G. X.; He, B. B.; Ma, W. L.; Sun, Y. F. Thermodynamic analysis based on simultaneous chemical and phase equilibrium for dehydration of glycerol with methanol. *Energy* **2019**, *188*, No. 116021.

(24) Pariente, S.; Tanchoux, N.; Fajula, F. Etherification of glycerol with ethanol over solid acid catalysts. *Green Chem.* **2009**, *11*, 1256−1261.

(25) Marinho, C. M.; Barrozo, M. A. D.; Hori, C. E. Optimization of glycerol etherification with ethanol in fixed bed reactor under various pressures. *Energy* **2020**, *207*, No. 118301.

(26) Lemos, C. O. T.; Rade, L. L.; Barrozo, M. A. D.; Cardozo, L.; Hori, C. E. Study of glycerol etherification with ethanol in fixed bed reactor under high pressure. *Fuel Process. Technol.* **2018**, *178*, 1−6.

(27) Hu, H. L.; Hu, D. X.; Jin, H. T.; Zhang, P. L.; Li, G. Z.; Zhou, H.; Yang, Y.; Chen, C. L.; Zhang, J.; Wang, L. Efficient Production of Furanic Diether in a Continuous Fixed Bed Reactor. *ChemSusChem* **2019**, *11*, 2179−2186.

(28) Mravec, D.; Turan, A.; Filkova, A.; Mikeskova, N.; Volkovicsova, E.; Onyestyak, G.; Harnos, S.; Lonyi, F.; Valyon, J.; Kaszonyi, A. Catalytic etherification of bioglycerol with bioethanol over h-beta, h-y and h-mor zeolites. *Fuel Process. Technol.* **2017**, *159*, 111−117.

(29) Estevez, R.; Lopez, M. I.; Jimenez-sanchidrian, C.; Luna, D.; Romero-salguero, F. J.; Bautista, F. M. Etherification of glycerol with tert-butyl alcohol over sulfonated hybrid silicas. *Appl. Catal., A* **2016**, *526*, 155−163.

(30) Cannilla, C.; Bonura, G.; Maisano, S.; Frusteri, L.; Migliori, M.; Giordano, G.; Todaro, S.; Frusteri, F. Zeolite-assisted etherification of glycerol with butanol for biodiesel oxygenated additives production. *J. Energy Chem.* **2020**, *48*, 136−144.

(31) Zhu, S. H.; Gao, X. Q.; Dong, F.; Zhu, Y. L.; Zheng, H. Y.; Li, Y. W. Design of a highly active silver-exchanged phosphotungstic acid catalyst for glycerol esterification with acetic acid. *J. Catal.* **2013**, *306*, 155−163.

(32) Yuan, Z. L.; Xia, S. X.; Chen, P.; Hou, Z. Y.; Zheng, X. M. Etherification of biodiesel-based glycerol with bioethanol over tungstophosphoric acid to synthesize glyceryl ethers. *Energy Fuels* **2011**, *25*, 3186−3191.

(33) Wang, Y. Q.; Zhao, D.; Wang, L. L.; Wang, X. Q.; Li, L. J.; Xing, Z. P.; Ji, N.; Liu, S. J.; Ding, H. Immobilized phosphotungstic acid based ionic liquid: Application for heterogeneous esterification of palmitic acid. *Fuel* **2018**, *216*, 364−370.

(34) Ma, T. L.; Ding, J. F.; Shao, R.; Xu, W.; Yun, Z. Dehydration of glycerol to acrolein over wells-dawson and keggin type phosphotungstic acids supported on mcm-41 catalysts. *Chem. Eng. J.* **2017**, *316*, 797−806.

(35) Sakthivel, R.; Kemnitz, E. Acetylation of anisole on TPA/ZrO2. *Indian J. Chem. Technol.* **2008**, *15*, 36−40.

(36) Singh, H.; Ali, A. Potassium and 12-tungstophosphoric acid loaded alumina as heterogeneous catalyst for the esterification as well as transesterification of waste cooking oil in a single pot. *Asia-Pac. J. Chem. Eng.* **2021**, *16*, No. e2585.

(37) Marosz, M.; Kowalczyk, A.; Chmielarz, L. Modified vermiculites as effective catalysts for dehydration of methanol and ethanol. *Catal. Today* **2020**, *355*, 466−475.

(38) Parida, K. M.; Mallick, S. Phosphotungstic acid promoted zirconia-alumina mixed oxides: a stable and reusable catalysts for epoxidation of trans-stilbene. *Catal. Commun.* **2009**, *11*, 51−57.

(39) Kong, X. J.; Wu, S. X.; Liu, L. Y.; Li, S.; Liu, J. H. Continuous synthesis of ethyl levulinate over cerium exchanged phosphotungstic acid anchored on commercially silica gel pellets catalyst. *Mol. Catal.* **2017**, *439*, 180−185.

(40) Gernhart, Z. C.; Anuja, B.; John, J. B.; Sonnenfeld, K. O.; Marin, C. M.; Richard, Z.; Cheung, C.Li. One-pot conversion of cellobiose to mannose using a hybrid phosphotungstic acid−cerium oxidecatalyst. *RSC Adv.* **2015**, *5*, 28478−28486.